Neuron, Vol. 17, 707–718, October, 1996, Copyright ©1996 by Cell Press

# Mutations in a Cyclic Nucleotide–Gated Channel Lead to Abnormal Thermosensation and Chemosensation in C. elegans

**Hidetoshi Komatsu,* Ikue Mori,* Jeong-Seop Rhee,† Norio Akaike,† and Yasumi Ohshima***
*Department of Biology
Faculty of Science
Kyushu University
Fukuoka 812-81
Japan
†Department of Physiology
Faculty of Medicine
Kyushu University
Fukuoka 812-82
Japan

## Summary

**The C. elegans *tax-4* mutants are abnormal in multiple sensory behaviors: they fail to respond to temperature or to water-soluble or volatile chemical attractants. We show that the predicted *tax-4* gene product is highly homologous to vertebrate cyclic nucleotide–gated channels. Tax-4 protein expressed in cultured cells functions as a cyclic nucleotide–gated channel. The green fluorescent protein (GFP)-tagged functional Tax-4 protein is expressed in thermosensory, gustatory, and olfactory neurons mediating all the sensory behaviors affected by the *tax-4* mutations. The Tax-4::GFP fusion is partly localized at the sensory endings of these neurons. The results suggest that a cyclic nucleotide–gated channel is required for thermosensation and chemosensation and that cGMP is an important intracellular messenger in C. elegans sensory transduction.**

## Introduction

Sensation of a variety of environmental stimuli induces diverse behavioral responses in animals. Mechanisms underlying sensation were well studied in some systems. Vertebrate photoreceptor and olfactory neurons are known to follow similar sequential molecular events in response to very different types of stimuli (light and an odor, respectively). In vision, light activates a G protein–coupled seven transmembrane protein, rhodopsin, which activates cascades for cGMP hydrolysis and decreases the intracellular cGMP concentration. A cyclic nucleotide–gated channel that had been kept open in the dark by being bound to cGMP then closes, leading to the hyperpolarization of the photoreceptor neurons (Fesenko et al., 1985). In olfaction, an odorant is thought to interact with a G protein–coupled seven transmembrane receptor, which activates pathways for cAMP synthesis (Pace et al., 1985; Sklar et al., 1986). The increased intracellular cAMP concentration then opens a cyclic nucleotide–gated channel, leading to the depolarization of the olfactory neurons (Nakamura and Gold, 1987; Kurahashi, 1990; Breer et al., 1990). Although generating different cellular responses, a cyclic nucleotide–gated channel serves as the final step in both visual and olfactory sensory transduction systems.

Cyclic nucleotide–gated channels are nonselective cation channels that belong to a family that includes voltage-gated channels (Jan and Jan, 1990). Vertebrate cyclic nucleotide–gated channels are likely to function as a hetero-oligomer and consist of at least two distinct subunits, $\alpha$ or subunit 1 and $\beta$ or subunit 2, in vivo (Cook et al., 1987; Kaupp et al., 1989; Dhallan et al., 1990, 1992; Chen et al., 1993; Bradley et al., 1994; Liman and Buck, 1994). Both subunits are homologous to each other and contain similar domains including a cyclic nucleotide–binding site on their cytoplasmic sides. In Drosophila, a single type of cyclic nucleotide–gated channel has been found in antennae and eyes (Baumann et al., 1994). Recent studies suggest that functions of cyclic nucleotide–gated channels are much more diverged and prevalent than previously thought (Yau, 1994). Several mammalian organs besides sensory cells contain cyclic nucleotide–gated channels that are functional when expressed in heterologous systems (Biel et al., 1994; Weyand et al., 1994). It is also becoming clear that, besides generating membrane potential by conducting $Na^+$ or $K^+$, the general role of cyclic nucleotide–gated channels is to regulate intracellular $Ca^{2+}$ concentration, which in turn controls several intracellular signal transduction cascades in sensory and nonsensory cells (Frings et al., 1995).

In the nematode Caenorhabditis elegans, chemosensation and thermosensation are two major sensory systems for the animals that ensure their survival in the natural environment. Detailed analysis of chemotaxis and related sensory responses showed that C. elegans can discriminate numerous volatile and water-soluble compounds (Bargmann and Horvitz, 1991a, 1991b; Bargmann et al., 1993). Like in vertebrates, the C. elegans olfactory and gustatory signal transductions are likely to be initiated by activations of G protein–coupled seven transmembrane receptors (Troemel et al., 1995; Sengupta et al., 1996).

Studies on thermotaxis indicate that C. elegans uses a thermal cue besides a rich repertoire of chemical cues to find and stay near its food source. Thermotaxis is a complex and interesting behavior in the sense that neuronal plasticity can be directly observed in the behavioral responses. After being cultivated normally on a plate seeded with bacteria (food) at a temperature ranging from 15°C to 25°C and placed on an unseeded plate with a temperature gradient, wild-type animals migrate to its cultivation temperature and stay around it by moving isothermally (Hedgecock and Russell, 1975; Mori and Ohshima, 1995; see Figures 1A–1C). A preferred temperature can be reset by cultivation with food at a new temperature for several hours (Hedgecock and Russell, 1975). Starvation is a key element that can strongly modulate thermotaxis: on a temperature gradient, the animals migrate away from the cultivation temperature at which they were unfed for only a few hours (Hedgecock and Russell, 1975; I. M. and Y. O., unpublished data). Thermotaxis can therefore provide a model

behavioral system to study thermosensation, sensory adaptation, thermal information storage, and possibly some form of learning (Mori and Ohshima, 1995). As one approach to understand these processes, we have isolated and analyzed mutants defective in thermotaxis behavior. Thermotaxis-defective mutants can be divided into three major phenotypic classes: they are cryophilic (cold-seeking), thermophilic (heat-seeking), or athermotactic (non-temperature-responsive) on a temperature gradient. Mutants can be further subdivided into two different phenotypic classes based on the ability to move isothermally on a temperature gradient (Hedgecock and Russell, 1975; Mori and Ohshima, 1995).

In C. elegans, chemosensory and thermosensory neurons have been functionally defined by killing individual cells in live animals through laser ablation and analysis of the resultant behavioral responses. Of 302 neurons in the nervous system of an adult C. elegans hermaphrodite, C. elegans uses two types of olfactory neurons (AWA and AWC) to detect volatile attractants and six types of gustatory neurons (ASE, ADF, ASG, ASI, ASK, and ASJ) to detect water-soluble attractants as well as dauer pheromone, which induces dauer larvae (White et al., 1986; Bargmann et al., 1993; Bargmann and Horvitz, 1991a, 1991b). A single type of thermosensory neuron, AFD, is essential to detect temperature (Mori and Ohshima, 1995). Additionally, coordinated regulation of the two types of interneurons, AIY and AIZ, is important for processing thermosensory signals to achieve thermotaxis (Mori and Ohshima, 1995). Sensory endings of these functionally defined chemosensory and thermosensory neurons participate to form the largest sensory organ, called amphid, which is localized as a bilaterally symmetric pair in the tip of the head (Ward et al., 1975; Ware et al., 1975).

Combined information obtained from behavioral, genetic, and cellular analyses of the C. elegans sensory behaviors should facilitate molecular dissection of these behaviors. We show here that the *tax-4* gene encodes a C. elegans homolog of an $\alpha$ subunit of a cyclic nucleotide–gated channel. *tax-4* mutants are athermotactic in thermotaxis, fail to respond to water-soluble and volatile attractants in chemotaxis, and are weakly defective in dauer formation. The expression pattern of the *tax-4::GFP* translational fusion gene suggests that a cyclic nucleotide–gated channel is required independently in thermosensory, gustatory, and olfactory neurons to direct sensations of diverse types of sensory stimuli. *tax-2* mutants show behavioral abnormalities almost identical to those of *tax-4* mutants, and the *tax-2* gene encodes a potential $\beta$ subunit of a cyclic nucleotide–gated channel (Coburn and Bargmann, 1996 [this issue of *Neuron*]). These results suggest that Tax-4 and Tax-2 form a hetero-oligomer in vivo that is required for thermosensation and chemosensation in C. elegans.

## Results

### *tax-4* Mutants Fail to Respond to Temperature, a Water-Soluble Attractant (NaCl), and AWC-Sensed Odorants

To identify genes required for thermotaxis, we carried out behavioral screens to isolate thermotaxis-defective mutants. When the wild-type animals were grown at a temperature of 15°C–25°C under normal conditions and then placed in a region of a linear temperature gradient that corresponds to the growth temperature, they mostly stay around the region where placed (Hedgecock and Russell, 1975). Using this assay system, we selected progeny of mutagenized animals that migrated abnormally to a region colder or warmer than the growth temperature.

Of newly isolated athermotactic mutations showing almost random movement on a temperature gradient, two mutations, *ks11* and *ks28*, as well as the previously isolated *tax-4(p678)* mutation (Dusenbery et al., 1975), failed to complement one another. These three mutations are all recessive, cause very similar athermotactic phenotype (Figures 1B and 1C), and map to the region near *lon-1* on chromosome III, suggesting that they affect the same gene, *tax-4*. The *tax-4(p678)* mutant is also known to be defective in chemotaxis to salts and some volatile attractants (Hedgecock and Russell, 1975; Dusenbery et al., 1975; Bargmann et al., 1993). To confirm these results, we analyzed three *tax-4* mutants for chemotaxis to NaCl and six volatile attractants. Salts are sensed primarily by the ASE gustatory neurons, and a variety of volatile attractants are sensed by either the AWA or AWC olfactory neurons, or both of these neurons (Bargmann and Horvitz, 1991a; Bargmann et al., 1993). In chemotaxis assay plates with the gradient of the NaCl concentration, all three *tax-4* mutants moved almost randomly and failed to migrate to the concentration peak, whereas over 80% of the wild-type animals migrated to the peak (Figure 1D and Table 1). In odorant responses, the three *tax-4* mutants failed to respond to the AWC-sensed odorants (benzaldehyde, 2-butanone, and isoamyl alcohol). However, they displayed nearly normal responses at the concentrations tested to the AWA-sensed odorants (diacetyl and pyrazine) and responded reasonably well to trimethylthiazole, which is detected by both AWA and AWC neurons (Figure 1E). These olfactory defects of *tax-4* mutants are consistent with the previous reports (Bargmann et al., 1993).

In addition to the thermotaxis and chemotaxis defects, the *tax-4* mutants are slightly abnormal in dauer formation (for review, see Riddle, 1988; Coburn et al., unpublished data; data not shown). When each *tax-4* mutation was combined with the *unc-31* mutation that is thought to affect all neuronal functions in C. elegans (Avery et al., 1993), over 90% of resultant *tax-4; unc-31* double mutants formed dauers under non-dauer-forming conditions (I. Katsura, personal communication; data not shown). Other behavioral responses in *tax-4* mutants are indistinguishable from those of wild-type animals. Their locomotion, mating, egg laying, feeding, and responses to mechanical stimuli appear to be normal, although they are slightly smaller and grow slightly slower than the wild-type animals.

### Molecular Cloning of the *tax-4* Gene

Using several three factor crosses and the sequence-tagged site (STS) mapping (Williams et al., 1992), *tax-4(ks11)* was localized to the region between *unc-32* and *emb-9*, and possibly near or to the right of *lin-12* (Figure

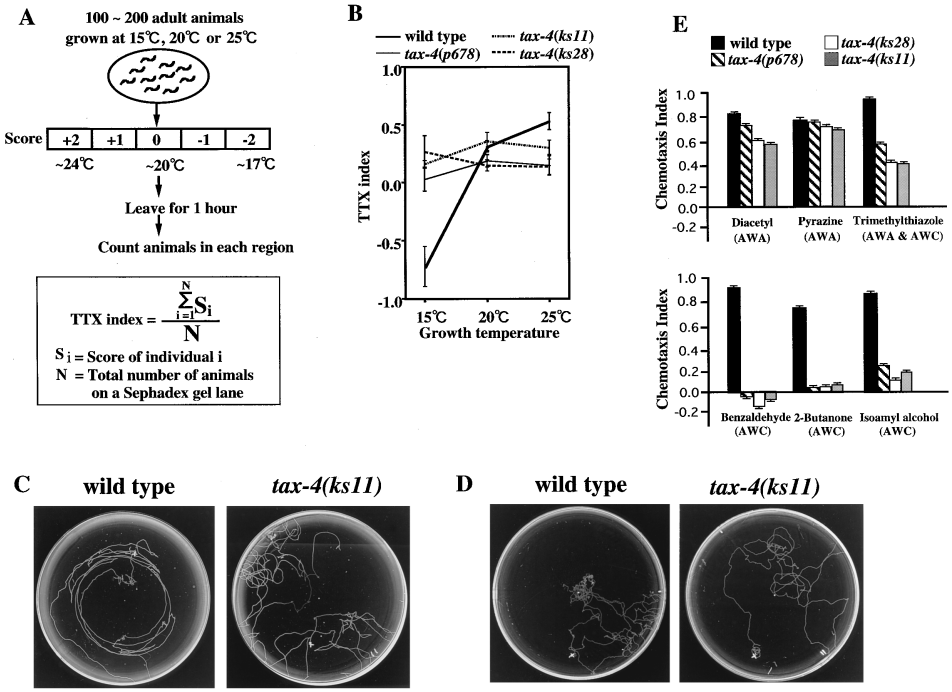


Figure 1. *tax-4* Mutants Are Defective in Multiple Sensory Behaviors

(A) A diagram showing the procedure for population thermotaxis assay on a linear temperature gradient. Approximately 100–200 animals that had been grown normally at 15°C, 20°C, or 25°C were washed with NG buffer three times to get rid of bacteria (food), and then applied onto the 20°C region of the gel slurry carrying a linear temperature gradient. After 1 hr, the animals in each of the five regions with score +2, +1, 0, −1, or −2 were counted. TTX index, the mean score of the animals in a gel lane, was then calculated as described.

(B) TTX indices of wild-type and three *tax-4* mutant strains grown at 15°C, 20°C, or 25°C. The wild-type animals migrated toward the growth temperature. The three *tax-4* mutant strains were almost insensitive to the growth temperature; regardless of the growth temperature, they moved toward colder as well as warmer temperatures, which led to the large variances of TTX indices (data not shown). Each TTX index data point represents the mean of four independent assays with standard error of mean (SEM) shown by an error bar.

(C) Tracks of wild-type and *tax-4(ks11)* worms showing thermotaxis behaviors on a radial temperature gradient. The wild-type animal moved isothermally around the growth temperature (20°C), which is indicated by clear isothermal tracks. By contrast, the *tax-4(ks11)* animal moved almost randomly and was severely defective in isothermal tracking.

(D) Tracks of wild-type and *tax-4(ks11)* worms showing chemotaxis behaviors on an agar plate with a concentration gradient of NaCl. While the wild-type animal migrated to the concentration peak at the center, the *tax-4(ks11)* mutant failed to respond to the concentration gradient.

(E) Odorant responses of wild-type and *tax-4* mutant animals. The assay procedures were according to Bargmann et al. (1993). The dilution of odorants were 1:10 for isoamyl alcohol, 1:100 for diacetyl, benzaldehyde, 2-butanone, 2,4,5-trymethylthiazole, and 10 mg/ml for pyrazine. Each bar represents the mean of four to eight independent assays with an error bar showing SEM.

2A). Cosmids located between *lin-12* and *emb-9* were injected into the *tax-4(ks11); lin-15(n765ts)* mutant together with the *lin-15(+)* gene as a marker to detect transgenic animals (Coulson et al., 1986, 1988; Mello et al., 1991; Huang et al., 1994). The resulting transgenic animals were tested for thermotaxis and chemotaxis to NaCl. Both F54G8 and R07A8 cosmids were found to rescue the defects of the *tax-4* mutants (Figure 2B). By testing various subclones from the region common to both cosmids, a 6 kb SmaI–SphI region was identified that rescued the *tax-4* defects (Figure 2C). According to the corresponding genomic sequence that had been already determined by the C. elegans sequencing consortium, this 6 kb region was likely to contain a single gene (Sulston et al., 1992; Wilson et al., 1994). Based on this putative *tax-4* gene sequence, the full-length *tax-4* cDNA was sequenced completely by using reverse transcription–polymerase chain reaction (RT–PCR). Like many other C. elegans genes, the *tax-4* transcript was *trans*-spliced at its 5′ end to the splice leader RNA SL1 (Huang and Hirsh, 1989; Krause and Hirsh, 1987) and ended with a 14 base poly(A) stretch after a consensus polyadenylation signal sequence AAUAAA. The *tax-4* cDNA is 2551 bp in length and encodes a predicted

Table 1. *tax-4* Mutants Are Defective in Chemotaxis to NaCl

| Strain | Number of Animals | Chemotaxis (+) | (+/−) | (−) | Fraction of Che(+) Animals |
|---|---|---|---|---|---|
| Wild type | 47 | 40 | 0 | 7 | 0.851 |
| *tax-4(p678)* | 60 | 2 | 4 | 54 | 0.033 |
| *tax-4(ks11)* | 60 | 1 | 6 | 53 | 0.017 |
| *tax-4(ks28)* | 60 | 0 | 3 | 57 | 0.0 |

One or two animals were assayed per chemotaxis assay plate. When the animal migrated repeatedly to the concentration peak or stayed at the peak during the assay, the animal was scored as Che(+). When the animal migrated to the peak only once or stayed very briefly at the peak, the animal was scored as Che(+/−). When the animal failed to migrate to or stay at the peak, the animal was scored as Che(−) (see Figure 1D).

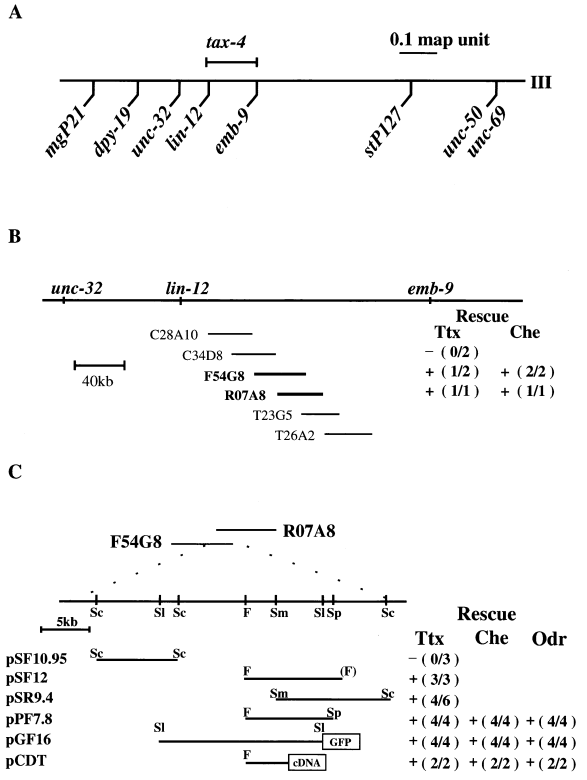


Figure 2. Genetic Location and Cloning of *tax-4*

(A) Genetic map position of the *tax-4* gene on the chromosome III. The positions of relevant marker genes and the Tc1 polymorphisms used for the mapping are shown.

(B) Identification of cosmids that rescued the *tax-4* defects. Cosmids corresponding to the *tax-4* region were injected into *tax-4(ks11); lin-15(n765ts)* animals. Transgenic lines were examined for the rescue of the thermotaxis and chemotaxis (NaCl) defects. F54G8 and R07A8 were found to rescue both defects. When the 20°C grown transgenic animals of a given line made clear isothermal circles around 20°C in a radial temperature gradient, the thermotaxis defect was regarded as rescued. When no animals (out of ~60) showed isothermal tracking, the thermotaxis defect was regarded as unrescued. When the fraction of Che(+) transgenic animals in a given line was 0.2–1.0, the chemotaxis defect was regarded as rescued. When the fraction of Che(+) transgenic animals was below 0.2, the chemotaxis defect was regarded as unrescued (see Table 1). The numbers in parentheses indicate the fraction of rescued lines. A plus sign indicates that at least one of the independent transgenic lines showed the rescue.

(C) Restriction map of the *tax-4* region and the rescue of the *tax-4* defects by various fragments. A 7.8 kb genomic fragment (pPF7.8), a *tax-4::GFP* translational fusion gene (pGF16), and *tax-4* cDNA under the endogenous *tax-4* promotor (pCDT) were able to rescue the defects in thermotaxis, chemotaxis to NaCl, and odorant response to benzaldehyde (see text and Experimental Procedures for the plasmid constructions). Rescue of thermotaxis and chemotaxis (NaCl) was evaluated as described in (B). Using the assay system established by Bargmann et al. (1993), chemotaxis to benzaldehyde was evaluated as follows. When the fraction of transgenic animals accumulating at the attractant source (A/A + C) was 0.7–1.0, the odorant response was regarded rescued. When the fraction (A/A + C) was below 0.7, the odorant response was regarded unrescued (A, the number of transgenic animals accumulating within 1.5 cm from a point source of benzaldehyde; C, the number of transgenic animals accumulating within 1.5 cm from a point source of ethanol, a control nonattractant). The numbers in the parentheses indicate the fraction of rescued lines. Abbreviations: Sc, SacI; Sl, SalI; F, FspI; Sm, SmaI; Sp, SphI. An FspI site in the parenthesis on pSF12 comes from the cosmid vector in F54G8.

protein of 733 amino acids (Figure 3A). The *tax-4* cDNA that we obtained is functionally complete, since the cDNA under the control of *tax-4* promoter (pCDT) rescued the *tax-4* defects (Figure 2C). By comparing sequences of the *tax-4* cDNA and the corresponding genomic region, we found that the *tax-4* gene includes ten exons and nine introns (Figure 3B). The 6 kb rescuing genomic region described above contains only about 1 kb sequence upstream of the initiating methionine for the predicted protein.

## Characterization of the Wild-Type and Mutant *tax-4* Genes

The predicted amino acid sequence of the *tax-4* gene product showed that it is highly homologous to a family of cyclic nucleotide–gated channels (Figure 4A). Like other cyclic nucleotide–gated channels, hydrophobicity analysis of Tax-4 protein revealed six hydrophobic peaks that could correspond to six membrane-spanning domains (H1–H6) (data not shown). The Tax-4 structure is somewhat unique in two aspects. First, the interval between the first and the second hydrophobic domains, H1 and H2, is 48 amino acids longer than those of other cyclic nucleotide–gated channels (Figure 4A). Second, the region between the $NH_2$-terminus and H1 has little homology with those of other channels. Despite these differences, Tax-4 protein shares 40% overall identity with the bovine and human rod photoreceptor channels, 37.3% identity with the Drosophila channel, 37% identity with the rat olfactory channel, and 38.3% identity with the catfish olfactory channel (Figure 4A). Particularly, the amino acid sequence of Tax-4 in the putative cyclic nucleotide–binding domain is highly homologous to those of other channels (66%–70% identity).

Several important structural features of vertebrate cyclic nucleotide–gated channels have been revealed through the electrophysiological analysis in heterologous systems. The amino acid sequence GNRRTAN, which is implicated in cyclic nucleotide selectivity for cGMP over cAMP, is absolutely conserved in all known cyclic nucleotide–gated channels and is also present in Tax-4 (Figure 4A; Altenhofen et al., 1991). An aspartic acid in the cyclic nucleotide–binding domains is conserved among rod photoreceptor channels and is thought to interact directly with N1 and N2 of cGMP through hydrogen bonds (Varnum et al., 1995). This aspartic acid is also present in the corresponding region of Tax-4 protein (Figure 4A, position 602). The histidine at position 420 of the bovine rod photoreceptor channel is thought to bind to $Ni^{2+}$, leading to the enhancement of the responses to both cGMP and cAMP (Figure 4A; Gordon and Zagotta, 1995a). Another histidine at position 394 of the rat olfactory channel is thought to bind to $Ni^{2+}$, leading to the inhibition of the olfactory channel (Gordon and Zagotta, 1995b). Both of these histidine residues are absent in Tax-4. Although cyclic nucleotide–gated channels display only a weak voltage dependence, Tax-4 contains a voltage sensor–like motif in the H4 domain like other cyclic nucleotide–gated channels (Figure 4B; Goulding et al., 1992). The H4 domain of voltage-gated channels such as $K^+$ channels has been proposed to serve as a voltage sensor. It consists of

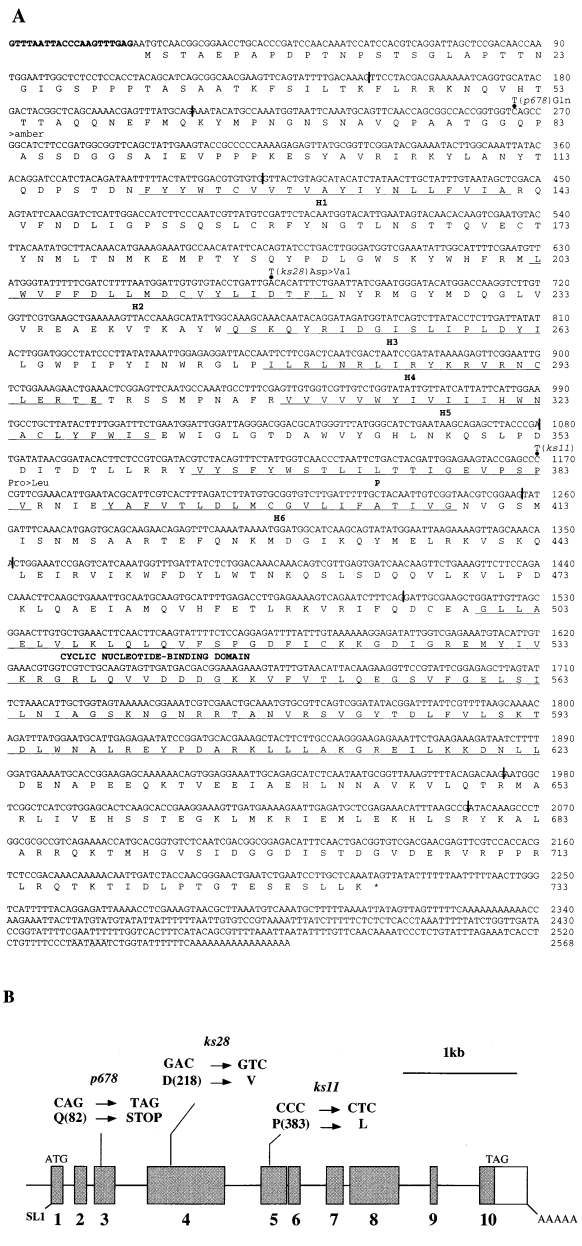


Figure 3. Sequence Analysis of *tax-4*

(A) Nucleotide sequence of the *tax-4* cDNA and predicted amino acid sequence. Splice junctions are marked by vertical lines. Mutation sites of *tax-4(p678)*, *tax-4(ks11)*, and *tax-4(ks28)* are indicated by dots with resultant amino acid substitutions. Nucleotides in bold characters at the 5′ end are derived from the *trans*-splice leader SL1 (Krause and Hirsh, 1987). A putative polyadenylation signal is boxed. The stop codon is marked by an asterisk. The putative transmembrane domains (H1–H6), the pore domain (P), and the cyclic nucleotide–binding domain are underlined.

(B) The schematic structure of the *tax-4* gene. Exons are boxed and numbered. Closed boxes and an open box show the coding regions and the 3′ noncoding region, respectively. Also shown are the *tax-4* mutation sites.

repeats of three amino acids: predominantly hydrophobic amino acid residues are found at every first and second position and positively charged arginine or lysine is found at every third position (Numa, 1989).

The entire *tax-4* coding regions of the three *tax-4* mutants were sequenced to identify important sites for the channel function. The *p678* mutation was a C-to-T transition that results in the conversion of glutamine (82) to a stop codon in the region near the $NH_2$-terminus, indicating that *p678* is a null mutation (Figure 3A). The *ks11* mutation was a C-to-T transition resulting in the substitution of proline (383) to leucine in the pore domain (Figure 3A). The proline residue at this position is absolutely conserved among all cyclic nucleotide–gated channels (Figure 4A). The *ks28* mutation was an A-to-T transversion resulting in the substitution of aspartic acid (218) to valine in the transmembrane domain H2 (Figure 3A). This aspartic acid is also highly conserved in all members of the cyclic nucleotide–gated channels (Figure 4A). The schematic structure of Tax-4 and the mutation sites are shown in Figure 4C.

## Tax-4 Functions as a Channel in Cultured Cells

The nearly identical hydrophobic profiles and the high level of overall homology with other cyclic nucleotide–gated channels suggest strongly that Tax-4 functions as a cyclic nucleotide–gated channel. To determine whether Tax-4 indeed exhibits a channel function, we transiently expressed Tax-4 in HEK293 cells (see Experimental Procedure). Electrophysiological analyses showed that Tax-4 can form a functional channel that is activated in response to cyclic nucleotide. Figure 5A shows representative examples of the cyclic nucleotide–induced macroscopic currents from inside-out patches of the transfected cells. The relationships between the currents and the cyclic nucleotide concentrations are shown in Figure 5B. The half-maximum effective concentration ($K_D$) and Hill coefficient (n) were calculated to be $4.1 \times 10^{-7}$ M and 0.93 for cGMP, and $1.4 \times 10^{-4}$ M and 1.6 for cAMP, respectively. The maximal cAMP-activated current was about 80% of that of cGMP-activated currents. When a macroscopic current–voltage (I–V) relationship for $10^{-5}$ M cGMP-induced currents was examined, a marked inward rectification was observed in potentials more negative than −60 mV, and a slight outward rectification was observed at potentials more positive than +60 mV. Consequently, the I–V relationships showed a sigmoidal fashion (Figure 5C). Previous studies also indicated such a sigmoidal I–V relationship of cyclic nucleotide–gated currents in Drosophila in the presence of extracellular $Ca^{2+}$ (Baumann et al., 1994). In addition, the average reversal potential in the present study was 18.4 ± 1.7 mV, which was higher (positive) than $Na^+$ equilibrium potential ($E_{Na}$) of 0 mV, indicating that Tax-4 channel is permeable not only to $Na^+$ but also to $Ca^{2+}$. This result is in good agreement with high $Ca^{2+}$ permeability of a cyclic nucleotide–gated channel in Drosophila (Baumann et al., 1994).

## Tax-4 Is Expressed in Sensory Neurons That Mediate Thermotaxis and Chemotaxis

Two models could explain the multiple sensory defects of *tax-4* mutants. Tax-4 protein might be required in the sensory neurons that mediate the sensory behaviors found to be affected by the *tax-4* mutation. Alternatively,

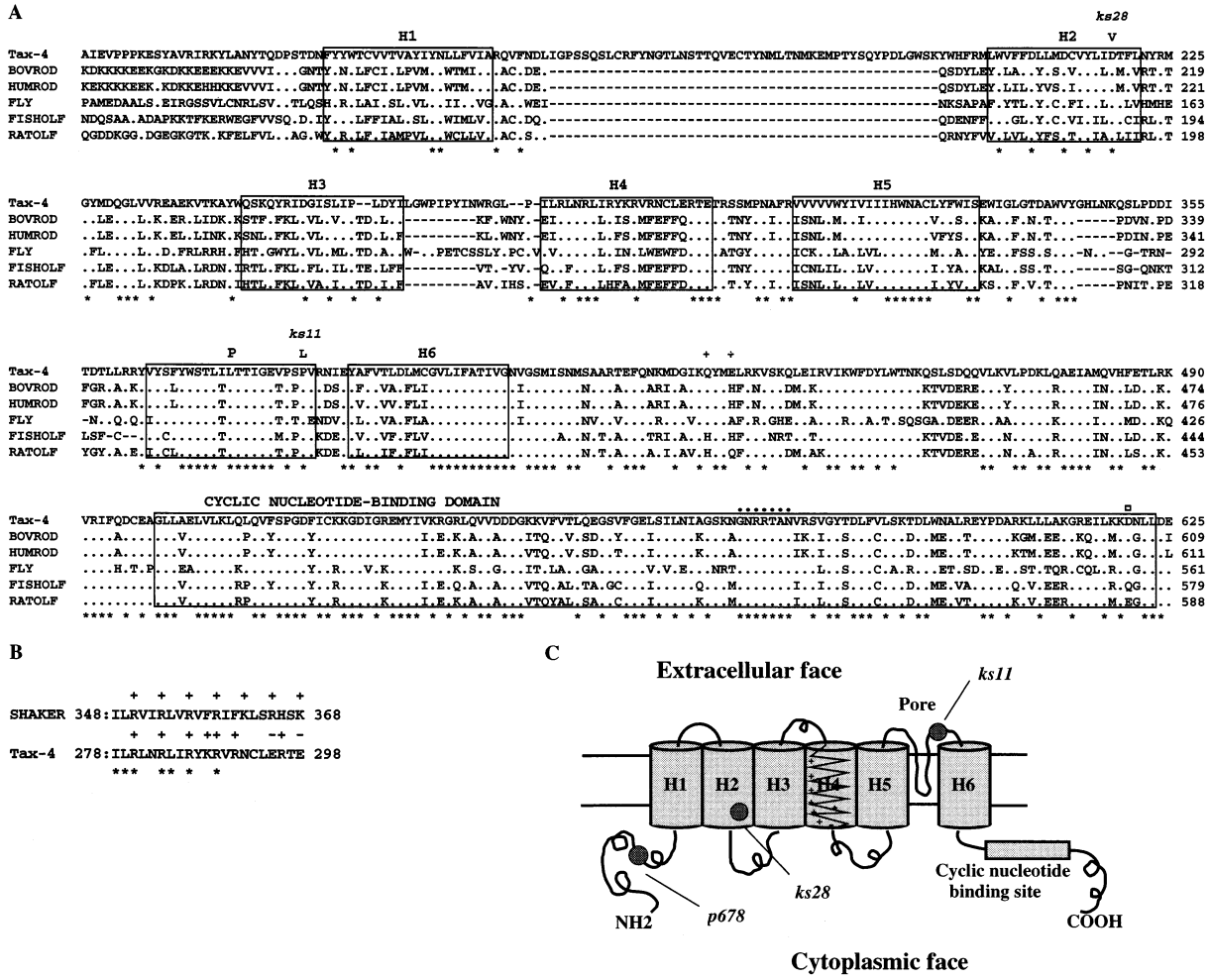


Figure 4. Homologies between Tax-4 and Other Cyclic Nucleotide–Gated Channels

(A) Alignment of amino acid residues of Tax-4 with those of other cyclic nucleotide–gated channels. The putative transmembrane domains (H1–H6), the pore domains (P), and the cyclic nucleotide–biding domains are boxed. The mutation sites for *tax-4(ks11)* and *tax-4(ks28)* are indicated with the resultant amino acid substitutions. Amino acid residues conserved in all the members are indicated by a star below the alignment. The seven conserved amino acid residues implicated for the selectivity of cGMP over cAMP in the putative nucleotide–binding domain are indicated by a row of dots above the alignment (see text). The aspartic acid conserved among rod and Drosophila channels in the putative nucleotide-binding domains is marked by an open square. The positions of two histidine residues that are conserved among rod or olfactory channels are indicated by a plus sign (see text). Other channels are shown using the following abbreviations: BOVROD, bovine rod channel (Kaupp et al., 1989); HUMROD, human rod channel (Dhallan et al., 1992); FLY, Drosophila channel (Baumann et al., 1994); FISHOLF, catfish olfactory channel (Goulding et al., 1992); RATOLF, rat olfactory channel (Dhallan et al., 1990).

(B) Alignment between the putative H4 domain of Tax-4 and the putative voltage sensor region of a *Shaker* $K^+$ channel (Pongs et al., 1988). Plus and minus signs indicate the charge of amino acid residues. The conserved amino acid residue is indicated by a star.

(C) A diagram showing the putative folding pattern of Tax-4. Mutation sites in *p678*, *ks28*, or *ks11* are shown.

Tax-4 protein might be necessary for downstream interneurons to receive, integrate, or process signals from sensory neurons involved in the affected sensory behaviors. To distinguish between these two models, we localized the *tax-4* gene expression. A green fluorescent protein (GFP) under the control of the *tax-4* promoter should serve as a reporter to detect the *tax-4* expression in live transgenic animals (Chalfie et al., 1994). The GFP gene was fused to the extreme COOH-terminus of the *tax-4* gene carrying 13 kb of upstream sequence, and the resultant construct (Figure 2C) was able to rescue the defects of the *tax-4* mutants in thermotaxis and chemotaxis to NaCl or benzaldehyde. The GFP expression was detected in cell bodies of sensory neurons including the AFD thermosensory neurons, the AWC olfactory neurons, and the ASE, ASG, ASK, ASI, and ASJ gustatory neurons (Figures 6A and 6B). These sensory neurons mediate thermotaxis, chemotaxis to water-soluble attractants, the AWC-sensed odorant responses, and dauer formation, all of which are affected by the *tax-4* mutations. These results are consistent with the model that the Tax-4 channel functions in the sensory neurons.

The C. elegans chemosensory and thermosensory neurons have specialized sensory endings that appear to be beneficial for sensing different types of stimuli (Ward et al., 1975; Ware et al., 1975). The gustatory

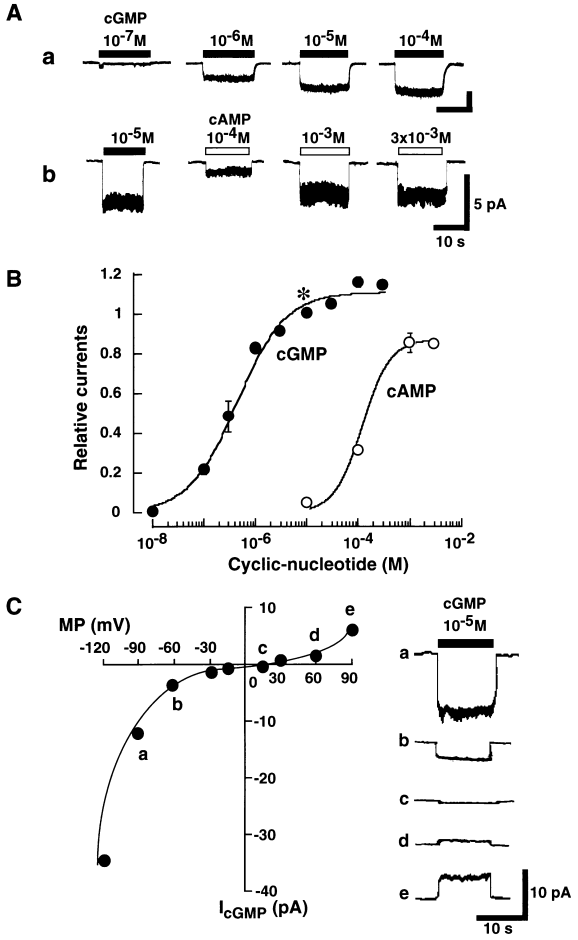


Figure 5. Electrophysiological Properties of Cyclic Nucleotide–Gated Channels Expressed in HEK293 Cells

(A) cGMP and cAMP induced currents in an inside-out membrane patch of HEK293 cells at a holding potential of −60 mV.

(B) Concentration–response relationships for cGMP- and cAMP-induced currents. All current responses to two kinds of cyclic nucleotides were normalized to that elicited by $10^{-5}$ M cGMP. The concentration–response curves were fitted by $I = I_{max} (C^n/(C^n + K_D^n))$, where I is current, C is the cyclic nucleotide concentration, $K_D$ is the half-maximum effective concentration, $I_{max}$ is the maximum response, and n is the Hill coefficient. Each point represents the mean ± SEM from four cells.

(C) A typical current–voltage (I–V) relationship for $10^{-5}$ M cGMP-induced currents. The symbols (a)–(e) in inset are indicated by the corresponding letters in I–V relationship.

neurons such as ASE have one or two long cilia directly exposed to the environment through the amphid pore. The olfactory neurons, AWA and AWC, have extensively branched cilia that are enclosed in the amphid sheath cell, but are partly exposed to the environment through the amphid pore. The AFD thermosensory neurons have many (about 40) finger-like projections that are embedded in the amphid sheath cell. If the Tax-4 cyclic nucleotide–gated channel is directly required for sensation, the GFP fluorescence would be expected to be seen at or near the sensory endings of the respective sensory neurons. In transgenic animals, the GFP fluorescence was actually detected near the tip of the head, a site that corresponds to the amphid sensory organ (Figures 6C and 6D). The fluorescence was also weakly visible in dendrites of the amphid sensory neurons (Figures 6A and 6D). No Tax-4::GFP fusion expression was observed in the axons. Since the amphid contains all sensory endings of the neurons mediating the *tax-4*-affected behaviors, this result suggests that the endogenous Tax-4 protein is localized at the sensory endings to direct sensations of diverse sensory stimuli.

## Discussion

### Tax-4 Is an α Subunit of a Cyclic Nucleotide–Gated Channel

Native vertebrate cyclic nucleotide–gated channels have been proposed to function as hetero-oligomers consisting of two homologous subunits, α and β (Chen et al., 1993; Bradley et al., 1994; Liman and Buck, 1994; Körschen et al., 1995). The α subunits have been extensively analyzed using electrophysiology, since they can form functional homooligomers in heterologous systems. Only a few β subunits have been identified to date, and their physiological properties can be analyzed only when coexpressed with the relevant α subunits. In this study, we demonstrated that Tax-4 alone can reconstitute a functional cyclic nucleotide–gated cation channel in a mammalian cell system, suggesting that Tax-4 functions as an α subunit in C. elegans. Consistent with this result, the homology of Tax-4 protein with the β subunits is lower than that with the α subunits: the amino acid identity of Tax-4 with the β subunit of the rat olfactory channel is 32% and that with the β (2b) subunit of the human rod photoreceptor channel is 21% (Bradley et al., 1994; Liman and Buck, 1994; Chen et al., 1993). The relatively high homology between Tax-4 and the β subunit of the rat olfactory channel may be related to the fact that the α and β subunits of the rat olfactory channels are highly homologous to each other (Bradley et al., 1994; Liman and Buck, 1994). The C. elegans *tax-2* mutants show great behavioral similarities with *tax-4* mutants (Coburn and Bargmann, 1996; Coburn et al., unpublished data; data not shown). The *tax-2* gene encodes a putative β subunit of a cyclic nucleotide–gated channel and could represent a potential molecular partner of the *tax-4* gene product (Coburn and Bargmann, 1996). Consistent with these results, the cells expressing the *tax-2* gene is almost identical to those expressing the *tax-4* gene, and the overexpression of the *tax-4* gene could rescue the defects of *tax-2* mutants (Coburn and Bargmann, 1996). As in vertebrate visual and olfactory systems, a cyclic nucleotide–gated channel is likely to function as a hetero-oligomer, consisting of Tax-4 and Tax-2, in the C. elegans thermosensory and chemosensory systems.

Electrophysiological analysis revealed important features of Tax-4 channel. Tax-4 channel was found to be functionally more similar to rod photoreceptor channels than olfactory channels (Gordon and Zagotta, 1995a). Tax-4 is about 300 times less sensitive to cAMP than to cGMP, and maximal currents ($I_{max}$) induced by cAMP is significantly lower (80%) than those induced by cGMP (Figures 5A and 5B). Consistent with this result, a putative cyclic nucleotide–binding domain of Tax-4 is more

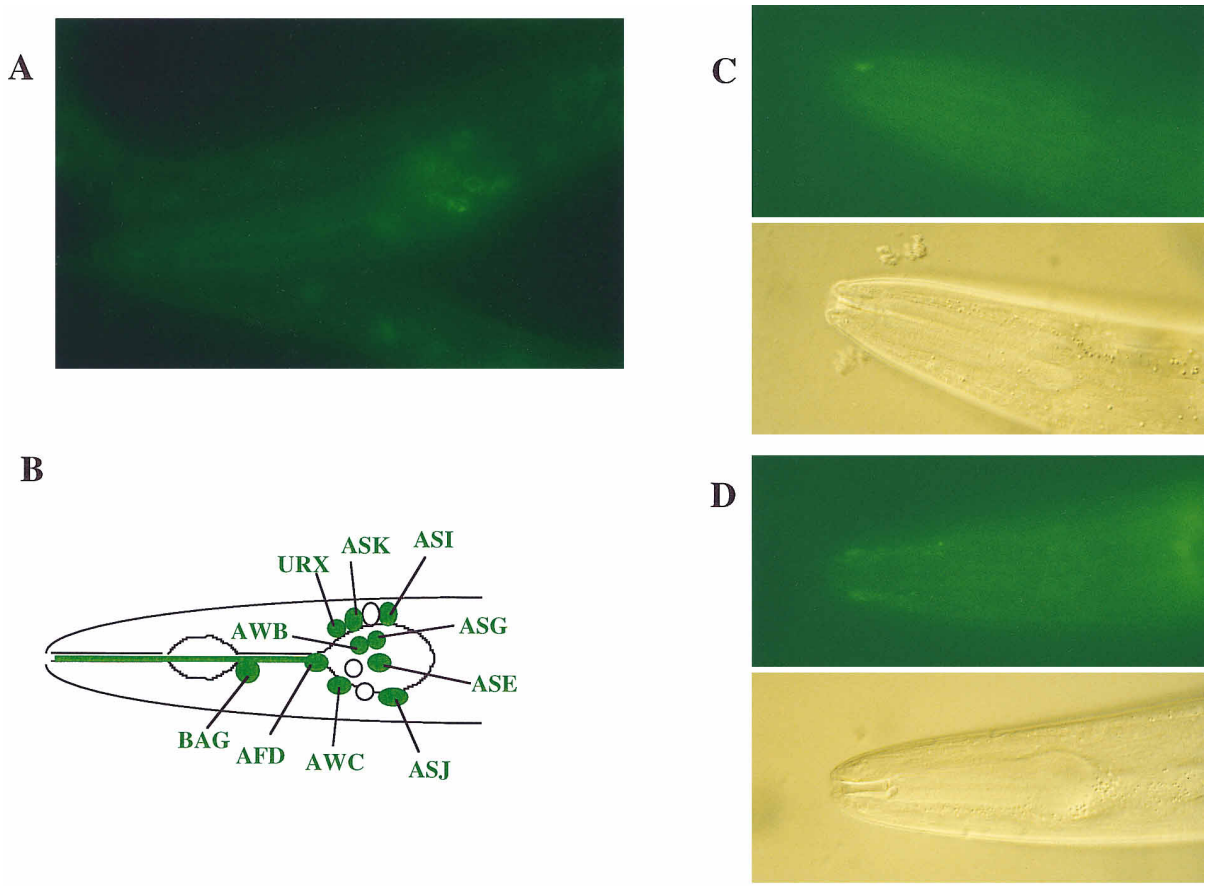


Figure 6. Localization of the GFP-Tagged Functional Tax-4 Protein

(A) Lateral view of an animal showing GFP expression in the head. GFP fluorescence is seen in the cell bodies of AFD, AWC, AWB, ASG, ASE, ASJ, and ASI neurons. Other GFP-expressing neurons (BAG, URX, and ASK) are in different focal planes. Weak expression of the Tax-4 protein is also visible in the dendrites of amphid sensory neurons. Anterior is to the left, and dorsal is up.

(B) A diagram summarizing the GFP-expressing neurons.

(C) Lateral view of an animal showing localization of the Tax-4 protein at the sensory endings in the right amphid. The Nomarski view of the same focal plane is shown below. Anterior is to the left, and ventral is up.

(D) Dorsal view of an animal showing localization of the Tax-4 protein at the sensory endings in both left and right amphids. GFP expression is also visible in a part of the dendrites near the sensory endings. The Nomarski view of the same focal plane is shown below. Anterior is to the left, and the left lateral side is up.

similar to those of rod photoreceptor channels (70%) than those of olfactory channels (67%). Also, Tax-4 contains the aspartic acid residue that is highly conserved among the cyclic nucleotide–binding domains of the rod photoreceptor channels (Varnum et al., 1995). Thus, in the actual physiological conditions, Tax-4 channel is likely to be activated only by cGMP. Perhaps, cGMP is used as an intracellular messenger in C. elegans and may regulate the activity of the Tax-4 channel in sensory neurons. Another important feature is that the Tax-4 channel displays a remarkable inward rectification at potentials lower than −60 mV (Figure 5C), which has not been reported in other known cyclic nucleotide–gated channels under similar experimental conditions.

### *tax-4* Is Expressed in Olfactory, Gustatory, and Thermosensory Neurons

The GFP-tagged functional Tax-4 protein was expressed in the sensory neurons mediating the behaviors that are abnormal in the *tax-4* mutants and was localized in sensory endings as well as in cell bodies and dendrites of these neurons (Figure 6). These results suggest that the native Tax-4 is directly required for sensation and for this reason is expressed in the sensory endings. This is also supported by analogy with the well established functions of cyclic nucleotide–gated channels in vertebrates. If Tax-4 is only involved in sensation for various sensory modalities, the abnormal axon outgrowth observed in some chemosensory neurons in the *tax-4* mutants (Coburn and Bargmann, 1996) could be an indirect consequence of the lowered sensory activity caused by the abnormal sensation. However, other possibilities for Tax-4 channel function also exist. The most plausible one is that Tax-4 might be directly required for both sensation and the axon outgrowth of chemosensory neurons. Consistent with this possibility, the GFP-tagged functional Tax-2 protein, a probable channel partner of Tax-4, was localized in sensory cilia as well as in the axons (Coburn and Bargmann, 1996). As implicated for vertebrate cyclic nucleotide–gated channels,

Tax-4 could be responsible for regulating the $Ca^{2+}$ entry, a role likely to be required for the correct axon outgrowth of chemosensory neurons (Frings et al., 1995). The observed Tax-4::GFP fluorescence in the cell bodies and the absence of the fluorescence in the axons (Figure 6A) might reflect inappropriate localization of the Tax-4::GFP fusion protein. In addition, the localization in the cell bodies might reflect the overexpression per se or possibly slow transport process of the native Tax-4 protein.

Molecular processes for C. elegans chemosensation are beginning to be revealed. Seven transmembrane domain receptors have been found in some of the olfactory and gustatory neurons of C. elegans, implying that the molecular events similar to those found in the vertebrate olfaction and vision could possibly be working in the C. elegans chemosensory systems (Troemel et al., 1995; Sengupta et al., 1996). The Odr-10 seven transmembrane receptors have been shown to be expressed in the AWA olfactory neurons (Sengupta et al., 1996), whose functions are essentially unaffected by *tax-4* mutations (Figure 1E). Thus, as in other vertebrate and invertebrate olfactory systems, cascades such as those involving $IP_3$ as an intracellular messenger may be mainly used in the AWA olfaction (Boekhoff et al., 1990, 1994; Breer et al., 1990). G proteins, G protein–coupled seven transmembrane receptors, and cyclic nucleotide hydrolysis are implicated in gustatory transduction in mammalian taste cells (McLaughlin et al., 1992; Ruiz-Avila et al., 1995; Kolesnikov and Margolskee, 1995). However, it is not yet known whether a cyclic nucleotide–gated channel is involved in any of the processes for the vertebrate gustatory sensation.

## Mechanism of Thermosensation

Despite its biological importance and interest, molecular mechanism of thermosensation is poorly understood in any metazoan. We demonstrated that a cyclic nucleotide–gated channel is required for thermotaxis behavior, providing a molecular clue to understand the mechanism of thermosensation. Unlike a subset of chemosensory neurons, the axon outgrowth of the AFD neurons is normal in the *tax-4* mutants at least at the microscopic level (J. Zallen and C. Bargmann, personal communication). These results led us to propose that the primary role of a cyclic nucleotide–gated channel in the AFD neurons is to direct thermosensation.

How is thermosensation achieved in C. elegans? Several hypotheses could be proposed. First, as the membrane fluidity is temperature dependent, the large membrane surface provided by the microvillus-like projections of the AFD neurons could be used to detect temperature. Second, temperature might be sensed by a thermoreceptor protein localized in the AFD projections. Precedents from two different systems support this second possibility. Light, a physical stimulus, is sensed by a conformational change of a chromophore retinal in the seven transmembrane domain protein, rhodopsin. In bacteria, four chemoreceptors all containing two transmembrane domains also function as thermoreceptors (Imae, 1985; Nara et al., 1991, 1996). In any case, a thermal signal received by a "thermoreceptor" may be transmitted to intracellular signal transduction cascades, and eventually to a cyclic nucleotide–gated channel through an intracellular messenger such as cGMP in the AFD neurons. Third, a cyclic nucleotide–gated channel per se could function as a thermoreceptor in the AFD neurons, since the state of the channels is generally known to be temperature dependent. It would be interesting to investigate whether a cyclic nucleotide–gated channel is expressed in thermosensory neurons of other species to direct thermosensation.

## Experimental Procedures

### Strains and Genetics

The techniques used for culturing C. elegans were essentially as described by Brenner (1974). The following strains were used in this work: wild-type C. elegans variety Bristol strain (N2), C. elegans variety Bergerac strain (RW7000), CB61 *dpy-5(e61)* I, CB3297 *vab-9(e1744)* II, *him-5(e1490)* V, FK151 *lon-1(e185) dpy-19(e1259ts)* III, CB2195 *dpy-19(e1259ts) unc-32(e189)* III, FK152 *dpy-19(e1259ts) unc-69(e587)* III, PR678 *tax-4(p678)* III, CB49 *unc-8(e49)* IV, CB4123 *lon-3(e2175)* V, CB1377 *daf-6(e1377)* X, CB678 *lon-2(e678)* X, DA589 *unc-32(e189) emb-9(hc70sd, ts, nn)* III, GS946 *unc-32(e189) lin-12(n137 n720)/qC1 [dpy-19(e1259ts) glp-1(q339)]* III, CB3657 *dpy-19(e1259ts) eP6 eP7 eP8 unc-50(e306)* III.

### Isolation of *tax-4(ks11)* and *tax-4(ks28)* Mutations

*tax-4(ks11)* and *tax-4(ks28)* were isolated in the screens to select animals that migrated abnormally on a linear temperature gradient. The procedure of selecting thermotaxis-defective mutants was according to Hedgecock and Russell (1975) with a slight modification. The wild-type strain (N2) or *daf-6(e1377)* (CB1377) strain was mutagenized using EMS and grown at 15°C, 20°C, or 23°C to generate the F2 progeny. The rationale to use chemotaxis-defective *daf-6* mutants for mutagenesis was to diminish the chemotaxis behaviors of the mutagenized animals during the thermotaxis screens. On a linear temperature gradient, the F2 animals were placed at the region of the Sephadex gel slurry (Sephadex G-200, superfine, Pharmacia), which corresponded to the growth temperature. After 1 hr, the animals that migrated to the region warmer or colder than the growth temperature were picked. The candidate mutants were assayed for thermotaxis with several generations to select real thermotaxis-defective mutants. In total, about 40,000 mutagenized genomes were screened, and *tax-4(ks11)* and *tax-4(ks28)* were isolated from the mutagenized *daf-6* and wild-type animals, respectively. Both mutants were outcrossed to the wild-type strain at least five times.

### Mapping of *tax-4*

By linkage analysis, *tax-4(ks11)* was found to be linked to *lon-1(e185)* on the chromosome III. The following mapping data indicated that *tax-4(ks11)* maps to the region between *unc-32* and *emb-9*, and possibly near or to the right of *lin-12* (Figure 2A). From *lon-1 dpy-19/tax-4(ks11)* hermaphrodites, 4 of 4 Lon-1 non-Dpy recombinant progeny segregated *tax-4*. From *dpy-19 unc-69/tax-4(ks11)* hermaphrodites, 6 of 9 non-Dpy Unc recombinant progeny segregated *tax-4*. From *dpy-19 unc-32/tax-4(ks11)* hermaphrodites, 0 of 8 non-Dpy Unc recombinant progeny segregated *tax-4*. From *unc-32 emb-9/tax-4(ks11)* hermaphrodites, 9 of 16 Unc non-Emb recombinant progeny segregated *tax-4*. From *unc-32 lin-12/tax-4(ks11)* hermaphrodites, 2 of 2 Unc non-Lin recombinant progeny segregated *tax-4*. From *dpy-19 unc-50/tax-4(ks11)* hermaphrodites, 1 of 11 Dpy non-Unc recombinant progeny segregated *tax-4*.

*tax-4* was also mapped using the method that utilizes the Tc1 polymorphisms (Williams et al., 1992). The *tax-4(ks11); him-5(e1490)* males were crossed with the hermaphrodites of the RW7000 strain. The F1 hermaphrodites were picked to separate plates and allowed to self. Among the progeny of these F1 hermaphrodites, the homozygous *tax-4(ks11)* animals were identified by thermotaxis assay, and their genomic DNA were tested for the presence or absence of the Bergerac Tc1s on the chromosome III by PCR. The mapping data based on the polymorphic Tc1 sites showed that *tax-4(ks11)* maps

to the region left of *stP127* and to the right of *mgP21* (*stP19* [14 of 32] *stP120* [3 of 32] *mgP21* [2 of 32] *tax-4* [1 of 32] *stP127* [12 of 32] *stP17*).

### Thermotaxis Assay

The procedure for the population thermotaxis assay using a linear thermal gradient was essentially according to Hedgecock and Russell (1975) with a slight modification (Figure 1A). The procedure for the thermotaxis assay using a radial temperature gradients was according to Mori and Ohshima (1995).

### Chemotaxis Assay

The procedure for assaying chemotaxis to NaCl was essentially according to Dusenbery et al. (1974) with some modification. A radial concentration gradients of NaCl was established by applying 2 μl of 5 M NaCl to the center of a 9 cm plate containing 8 ml of agar medium (2% agar, 0.25% Tween 20, 10 mM HEPES [pH 7.2]), and leaving the plates at room temperature for 12–16 hr. For assays, the animals were placed on the surface of agar 1 cm distant from the periphery and allowed to move freely for approximately 1–1.5 hr.

The procedure for assaying chemotaxis to odorants was according to Bargmann et al. (1993), except that the assay plates contained a slightly different medium (2% agar, 10 mM $MgSO_4$, 10 mM $CaCl_2$, 25 mM potassium phosphate). Chemotaxis indices were calculated according to Bargmann et al. (1993).

### Germline Transformation

Germline transformation was performed by coinjecting test DNA at a concentration of approximately 10–30 ng/μl and pJM23 (*lin-15*) DNA at a concentration of 50 ng/μl into the gonad of *tax-4(ks11); lin-15(n765ts)* animals (Mello et al., 1991; Huang et al., 1994). Transgenic animals were recognized by the rescue of the *lin-15* multivulval phenotype at 25°C. Multiple independent transgenic lines were established from each transformation and assayed for the rescue of the *tax-4* defects.

### Molecular Biology

Standard methods for molecular biology were used (Sambrook et al., 1989). All cosmid subcloning were done using pBluescript or pUC19. Subclones of F54G8 and R07A8 were generated as follows: F54G8 was digested with SacI to generate pSF10.95 and with FspI to generate pSF12. One of the FspI sites of pSF12 was from the vector sequence (see Figure 2C). R07A8 was digested with SmaI and SacI to generate subclone pSR9.4. pSF12 was digested with PstI (a polylinker site in pBluescript) and SphI to generate pPF7.8. Using pPD49.26 vector (Fire et al., 1990), the *tax-4* cDNA was allowed to be expressed under the control of the *tax-4* promotor (pCDT). The full-length *tax-4* cDNA and the 3 kb *tax-4* promoter region were both amplified by PCR. The sequence of the amplified cDNA was verified by sequencing.

### Characterization of cDNAs and Identification of Mutation Sites

Genomic DNA and RNA from a mixed population of wild-type (strain N2) and *tax-4* mutant animals were prepared as described by Sambrook et al. (1989). On the basis of the sequence of *tax-4* genomic region (ZC84.2) (Sulston et al., 1992), we synthesized oligonucleotides to sequence the open reading frames by PCR or RT–PCR. The primers used were as follows: upstream of coding sequence, CAAATTCCGAGTTTTTGATCCC; exon 1, GGAACCTGCACCCGAT CCAA; exon 3, CTCTTTTGGGGGCGGTACTT; exon 4, AACGATTG GGAAGATGGTCC, GGACGTGTGTGGTTACTGTA, CGGATTAGTCG ATTGAGTCG, and TACTTGGATGGCCTATCCCT; exon 7, TGTTGAT CACTCAACGACTG and CAACTGGAAATCCGAGTCATC; exon 8, CGTGCATCCGGATATTCTCT and TGCAAATGTGCGTTCAGTCG; exon 9, ACAAGAATGGCTCGGCTCAT; exon 10, GATTCAGTTCCCG TTGGTAG; downstream of coding sequence, TTAAGCGTTACTTTC GAGGT.

The 5′ end of mRNA was determined by RT–PCR analysis with SL1 splice-leader sequence primer (GGTTTAATTACCCAAGTTT GAG) and SL2 primer (GGTTTTAACCCAGTTACTCAAG). The PCR products were sequenced to confirm that they contained *tax-4* sequences. No PCR products were detected for reactions amplified with SL2. The 3′ end was determined by use of a variation of the 3′ RACE method described by Frohman et al. (1988).

### Expression of the *tax-4::GFP* Translational Fusion Gene

A SalI–SalI fragment that contained the *tax-4* genomic region and was derived from the cosmid F54G8 was ligated into the GFP expression vector *Tu#62* (Chalfie et al., 1994). The GFP translational fusion construct pGF16 and pJM23 (*lin-15* DNA) were coinjected into the gonads of *tax-4(ks11); lin-15(n765ts)* animals. Once the transformant lines were established, the animals were tested for the rescue of the *tax-4* defects and observed under the fluorescent microscopy for the GFP expression.

### Electrophysiology

The complete *tax-4* cDNA was inserted into the polylinker site of pCI (Promega) and pcDNAI/Amp (Invitrogen). HEK293 cells growing in DMEM with 10% FCS, 10% $CO_2$ were transfected with either one of the expression constructs and pCA-GFP(S65A) by calcium phosphate coprecipitation (Chen and Okayama, 1987). pCA-GFP(S65A) contains GFP(S65A) under the control of the cytomegalovirus enhancer–chicken β-actin hybrid promotor (Moriyoshi et al., 1996; Niwa et al., 1991). In the transfection with pcDNAI/Amp–*tax-4* cDNA, SV40 T-antigen expression vector pEF321-T was also transfected to achieve a higher level of expression (Dhallan et al., 1990). Patch-clamp recordings were made from the GFP-expressed cells 2–3 days after transfection.

Electrical recordings were performed in the excised patch recording inside-out mode (Hamill et al., 1981) at room temperature (21°C–24°C). The pipette solution contained 150 mM NaCl, 1 mM $CaCl_2$, and 10 mM HEPES (pH 7.4). The cytoplasmic face of the inside-out preparation was exposed to a solution consisting of 145 mM NaCl, 1 mM $CaCl_2$, 5 mM EGTA, 10 mM HEPES (pH 7.4). The current and voltage were measured with a patch-clamp amplifier (EPC-7, List-medical, Federal Republic of Germany) and were monitored on both a storage oscilloscope (MS-5100A, Iwatsu, Japan) and a pen recorder (RECTI-HORIZ-8K, Sanei, Japan), and were stored on video tapes after being digitized with a digital audio-processor (PCM-501-ESN, Nihon-Kohden, Japan). Rapid solution change was made with the "Y-tube" method as described elsewhere (Murase et al., 1990).

### Acknowledgments

We thank A. Coulson and R. Shownkeen for cosmids; the C. elegans sequencing consortium for unpublished genome sequence data; A. Fire and M. Chalfie for the GFP expression vector; I. Greenwald, L. Avery, and G. Stanfield for strains to map the *tax-4* mutations; P. Sengupta for plasmid pJM23 and the *lin-15(n765)* strain; K. Moriyoshi and J. Miyazaki for pCA-GFP(S65A) vector; C. Coburn and C. Bargmann for sharing unpublished results on *tax-2*; I. Katsura, T. Ishihara, J. Zallen, and C. Bargmann for strains and communicating unpublished data; C. Bargmann, T. Ishihara, I. Katsura, T. Kurahashi, K. Ogura, M. Koga, A. K. Azad, J. Park, H. Inada, M. Ishizaka, Y. Sakube, T. Hori, H. Ishibashi, M. Obana, T. Muta, and I. Ito for discussion and technical advice; C. Bargmann for comments on this manuscript. Some nematode strains used in this study were provided by the Caenorhabditis Genetics Center, which is funded by the National Institutes of Health National Center for Research Resources. This work was supported by the Human Frontier Science Program Organization (to I. M.), the Science and Technology Agency of Japan (to Y. O), and the Ministry of Education, Science, Sports and Culture of Japan (to I. M. and Y. O).

The costs of publication of this article were defrayed in part by the payment of page charges. This article must therefore be hereby marked *"advertisement"* in accordance with 18 USC Section 1734 solely to indicate this fact.

Received July 25, 1996; revised September 23, 1996.

### References

Altenhofen, W., Ludwig, J., Eismann, E., Kraus, W., Bönigk, W., and Kaupp, U.B. (1991). Control of ligand specificity in cyclic nucleotide–

gated channels from rod photoreceptors and olfactory epithelium. Proc. Natl. Acad. Sci. USA *88*, 9868–9872.

Avery, L., Bargmann, C.I., and Horvitz, H.R. (1993). The *Caenorhabditis elegans unc-31* gene affects multiple nervous system–controlled functions. Genetics *134*, 455–464.

Bargmann, C.I., and Horvitz, H.R. (1991a). Chemosensory neurons with overlapping functions direct chemotaxis to multiple chemicals in C. elegans. Neuron *7*, 729–742.

Bargmann, C.I., and Horvitz, H.R. (1991b). Control of larval development by chemosensory neurons in *Caenorhabditis elegans*. Science *251*, 1243–1246.

Bargmann, C.I., Hartwieg, E., and Horvitz, H.R. (1993). Odorant-selective genes and neurons mediate olfaction in C. elegans. Cell *74*, 515–527.

Baumann, A., Frings, S., Godde, M., Seifert, R., and Kaupp, U.B. (1994). Primary structure and functional expression of a *Drosophila* cyclic nucleotide–gated channel present in eyes and antennae. EMBO J. *13*, 5040–5050.

Biel, M., Zong, X., Distler, M., Bosse, E., Klugbauer, N., Murakami, M., Flockerzi, V., and Hofmann, F. (1994). Another member of the cyclic nucleotide–gated channel family, expressed in testis, kidney, and heart. Proc. Natl. Acad. Sci. USA *91*, 3505–3509.

Boekhoff, I., Tareilus, E., Strotmann, J., and Breer, H. (1990). Rapid activation of alternative second messenger pathways in olfactory cilia from rats by different odorants. EMBO. J. *9*, 2453–2458.

Boekhoff, I., Michel, W., Breer, H., and Ache, B. (1994). Single odors differentially stimulate dual second messenger pathways in lobster olfactory receptor cells. J. Neurosci. *14*, 3304–3309.

Bradley, J., Li, J., Davidson, N., Lester, H.A., and Zinn, K. (1994). Heteromeric olfactory cyclic nucleotide–gated channels: a subunit that confers increased sensitivity to cAMP. Proc. Natl. Acad. Sci. USA *91*, 8890–8894.

Breer, H., Boekhoff, I., and Tareilus, E. (1990). Rapid kinetics of second messenger formation in olfactory transduction. Nature *345*, 65–68.

Brenner, S. (1974). The genetics of *Caenorhabditis elegans*. Genetics *77*, 71–94.

Chalfie, M., Tu, Y., Euskirchen, G., Ward, W.W., and Prasher, D.C. (1994). Green fluorescent protein as a marker for gene expression. Science *263*, 802–805.

Chen, C., and Okayama, H. (1987). High-efficiency transformation of mammalian cells by plasmid DNA. Mol. Cell. Biol. *7*, 2745–2752.

Chen, T.-Y., Peng, Y.W., Dhallan, R.S., Ahamed, B., Reed, R.R., and Yau, K.W. (1993). A new subunit of the cyclic nucleotide–gated channel in retinal rods. Nature *362*, 764–767.

Coburn, C.M., and Bargmann, C.I. (1996). A putative cyclic nucleotide–gated channel is required for sensory development and function in C. elegans. Neuron *17*, this issue.

Cook, N.J., Hanke, W., and Kaupp, U.B. (1987). Identification, purification, and functional reconstitution of the cyclic GMP-dependent channel from rod photoreceptors. Proc. Natl. Acad. Sci. USA *84*, 585–589.

Coulson, A.R., Sulston, J., Brenner, S., and Karn, J. (1986). Towards a physical map of the genome of the nematode *Caenorhabditis elegans*. Proc. Natl. Acad. Sci. USA *83*, 7821–7825.

Coulson, A.R., Waterston, R., Kiff, J., Sulston, J., and Kohara, Y. (1988). Genome linking with yeast artificial chromosomes, Nature *335*, 184–186.

Dhallan, R.S., Yau, K.-W., Schrader, K.A., and Reed, R.R. (1990). Primary structure and functional expression of a cyclic nucleotide–activated channel from olfactory neurons. Nature *347*, 184–187.

Dhallan, R.S., Macke, J.P., Eddy, R.L., Shows, T.B., Reed, R.R., Yau, K.-W., and Nathans, J. (1992). Human rod photoreceptor cGMP-gated channel: amino acid sequence, gene structure, and functional expression. J. Neurosci. *12*, 3248–3256.

Dusenbery, D.B., Sheridan, R.E., and Russell, R.L. (1975). Chemotaxis-defective mutants of the nematode *Caenorhabditis elegans*. Genetics *80*, 297–309.

Fesenko, E., Kolesnikov, S., and Lyubarsky, A. (1985). Induction by cGMP of cationic conductance in plasma membrane of retinal rod outer segment. Nature *313*, 310–313.

Fire, A., Harrison, S.W., and Dixon, D. (1990). A modular set of *lac-Z* fusion vectors for studying gene expression in *Caenorhabditis elegans*. Gene *93*, 189–198.

Frings, S., Seifert, R., Godde, M., and Kaupp, U.B. (1995). Profoundly different calcium permeation and blockage determine the specific function of distinct cyclic nucleotide–gated channels. Neuron *15*, 169–179.

Frohman, M.A., Dish, M.K., and Martin, G.R. (1988). Rapid production of full-length cDNAs from rare transcripts: amplification using a single gene-specific oligonucleotide primer. Proc. Natl. Acad. Sci. USA *85*, 8998–9002.

Gordon, S.E., and Zagotta, W.N. (1995a). A histidine residue associated with the gate of the cyclic nucleotide–activated channels in rod photoreceptors. Neuron *14*, 177–183.

Gordon, S.E., and Zagotta, W.N. (1995b). Localization of regions affecting an allosteric transition in cyclic nucleotide–activated channels. Neuron *14*, 857–864.

Goulding, E.H., Ngai, J., Kramer, R.H., Colicos, S., Axel, R., Siegelbaum, S.A., and Chess, A. (1992). Molecular cloning and single-channel properties of the cyclic nucleotide–gated channel from catfish olfactory neurons. Neuron *8*, 45–58.

Hamill, O.P., Marty, A., Neher, E., Sakmann, B., and Sigworth, F.J. (1981). Improved patch-clamp techniques for high resolution current recording from cells and cell free membrane patches. Pflügers Arch. *391*, 85–100.

Hedgecock, E.M., and Russell, R.L. (1975). Normal and mutant thermotaxis in the nematode *Caenorhabditis elegans*. Proc. Natl. Acad. Sci. USA *72*, 4061–4065.

Huang, L.S., Tzou, P., and Sternberg, P.W. (1994). The *lin-15* locus encodes two negative regulators of *Caenorhabditis elegans* vulval development. Mol. Biol. Cell *5*, 395–412.

Huang, X., and Hirsh, D. (1989). A second trans-spliced RNA leader sequence in the nematode *Caenorhabditis elegans*. Proc. Natl. Acad. Sci. USA *86*, 8640–8644.

Imae, Y. (1985). Molecular mechanism of thermosensing in bacteria. In Sensing and Response in Microorganisms, M. Eisenbach and M. Balaban, eds. (New York: Elselvier Science Publishing, Incorporated), pp. 73–81.

Jan, L.Y., and Jan, Y.N. (1990). A superfamily of ion channels. Nature *345*, 672.

Kaupp, U.B., Niidome, T., Tanabe, T., Terada, S., Bönigk, W., Stühmer, W., Cook, N.J., Kanagawa, K., Matsuo, H., Hirose, T., Miyata, T., and Numa, S. (1989). Primary structure and functional expression from complementary DNA of the rod photoreceptor cyclic GMP-gated channel. Nature *342*, 762–766.

Kolesnikov, S.S., and Margolskee, R.F. (1995). A cyclic-nucleotide-suppressible conductance activated by transducin in taste cells. Nature *376*, 85–88.

Körschen, H.G., Illing, M., Seifert, R., Sesti, F., Williams, A., Gotzes, S., Colville, C., Müller, F., Dose, A., Godde, M., Molday, L., Kaupp, U.B., and Molday, R.S. (1995). A 240 kDa protein represents the complete β subunit of the cyclic nucleotide–gated channel from rod photoreceptor. Neuron *15*, 627–636.

Krause, M., and Hirsh, D. (1987). A trans-spliced leader sequence on actin mRNA in C. elegans. Cell *49*, 753–761.

Kurahashi, T. (1990). The response induced by intracellular cyclic AMP in isolated olfactory receptor cells of the newt. J. Physiol. *430*, 355–371.

Liman, E.R., and Buck, L.B. (1994). A second subunit of the olfactory cyclic nucleotide–gated channel confers high sensitivity to cAMP. Neuron *13*, 611–621.

McLaughlin, S.K., McKinnon, P.J., and Margolskee, R.F. (1992). Gustducin is a taste-cell-specific G protein closely related to the transducins. Nature *357*, 563–569.

Mello, C.C., Kramer, J.M., Stinchcomb, D., and Ambros, V. (1991).

Efficient gene transfer in *C. elegans*: extrachromosomal maintenance and integration of transforming sequences. EMBO J. *10*, 3959–3970.

Mori, I., and Ohshima, Y. (1995). Neural regulation of thermotaxis in *Caenorhabditis elegans*. Nature *376*, 344–348.

Moriyoshi, K., Richards, L.J., Akazawa, C., O'Leary, D.D.M., and Nakanishi, S. (1996). Labeling neural cells using adenoviral gene transfer of membrane-targeted GFP. Neuron *16*, 255–260.

Murase, K., Randic, M., Shirasaki, T., Nakagawa, T., and Akaike, N. (1990). Serotonin suppresses N-methyl-D-aspartate responses in acutely isolated spinal dorsal horn neurons of the rat. Brain Res. *525*, 84–91.

Nakamura, T., and Gold, G.H. (1987). A cyclic-nucleotide-gated conductance in olfactory receptor cillia. Nature *325*, 442–444.

Nara, T., Lee, L., and Imae, Y. (1991). Thermosensing ability of Trg and Tap chemoreceptors in *Escherichia coli*. J. Bacteriol. *173*, 1120–1124.

Nara, T., Kawagishi, I., Nishiyama, S., Homma, M., and Imae, Y. (1996). Modulation of the thermosensing profile of the *Escherichia coli* aspartate receptor Tar by covalent modification of its methy-accepting sites. J. Biol. Chem. *271*, 17932–17936.

Niwa, H., Yamamura, K., and Miyazaki, J. (1991). Efficient selection for high-expression transfectants with a novel eukaryotic vector. Gene *108*, 193.

Numa, S. (1989). A molecular view of neurotransmitter receptors and ionic channels. Harvey Lect. *83*, 121–165.

Pace, U., Hanski, E., Salomon, Y., and Lancet, D. (1985). Odorant-sensitive adenylate cyclase may mediate olfactory reception. Nature *316*, 255–258.

Pongs, O., Kecskemethy, N., Müller, R., Krah-Jentgens, I., Baumann, A., Kiltz, H.H., Canal, I., Llamazares, S., and Ferrus, A. (1988). *Shaker* encodes a family of putative potassium channel proteins in the nervous system of *Drosophila*. EMBO J. *7*, 1087–1096.

Riddle, D.L. (1988). The dauer larva. In The Nematode *Caenorhabditis elegans*, B.W. Wood, ed. (Cold Spring Harbor, New York: Cold Spring Harbor Laboratory Press), pp. 393–412.

Ruiz-Avila, L., McLaughlin, S.K., Wildman, D., McKinnon, P.J., Robichon, A., Spickofsky, N., and Margolskee, R.F. (1995). Coupling of bitter receptor to phosphodiesterase through transducin in taste receptor cells. Nature *376*, 80–85.

Sambrook, J., Fritsch, E.F., and Maniatis, T. (1989). Molecular Cloning: A Laboratory Manual (Cold Spring Habor, New York: Cold Spring Habor Laboratory Press).

Sengupta, P., Chou, J.H., and Bargmann, C.I. (1996). *odr-10* encodes a seven transmembrane domain olfactory receptor required for responses to the odorant diacetyl. Cell *84*, 899–909.

Sklar, P.B., Anholt, R.R.H., and Snyder, S.H. (1986). The odorant-sensitive adenylate cyclase of olfactory receptor cells: differential stimulation by distinct classes of odorants. J. Biol. Chem. *261*, 25538–25543.

Sulston, J., Du, Z., Thomas, K., Wilson, R., Hillier, L., Staden, R., Halloran, N., Green, P., Thierry-Mieg, J., Qiu, L., Drear, S., Coulson, A., Craxton, M., Durbin, R., Berks, M., Metzstein, M., Hawkins, T., Ainscough, R., and Waterson, R. (1992). The *C. elegans* genome sequencing project: a beginning. Nature *365*, 37–41.

Troemel, E.R., Chou, J.H., Dwyer, N.D., Colbert, H.A., and Bargmann, C.I. (1995). Divergent seven transmembrane receptors are candidate chemosensory receptors in C. elegans. Cell *83*, 207–218.

Varnum, M.D., Black, K.D., and Zagotta, W.N. (1995). Molecular mechanism for ligand discrimination of cyclic nucleotide–gated channels. Neuron *15*, 619–625.

Ward, S., Thomson, N., White, J.G., and Brenner, S. (1975). Electron microscopical reconstruction of the anterior sensory anatomy of the nematode *Caenorhabditis elegans*. J. Comp. Neurol. *160*, 313–337.

Ware, R.W., Clark, D., Crossland, K., and Russell, R.L. (1975). The nerve ring of the nematode *Caenorhabditis elegans*: sensory input and motor output. J. Comp. Neurol. *162*, 71–110.

Weyand, I., Godde, M., Frings, S., Weiner, J., Müller, F., Altenhofen, W., Hatt, H., and Kaupp, U.B. (1994). Cloning and functional expression of a cyclic-nucleotide-gated cahnnel from mammalian sperm. Nature *368*, 859–863.

White, J.G., Southgate, E., Thomson, J.N., and Brenner, S. (1986). The structure of the nervous system of the nematode *Caenorhabditis elegans*. Phil. Trans. Roy. Soc. (Lond.) B *314*, 1–340.

Williams, B.D., Schrank, B., Huynh, C., Shownkeen, R., and Waterston, R.H. (1992). A genetic mapping system in *Caenorhabditis elegans* based on polymorphic sequence-tagged sites. Genetics *131*, 609–624.

Wilson, R., Ainscough, R., Anderson, K., Baynes, C., Barks, M., Bonfield, J., et al. (1994). 2.2 Mb of contiguous nucleotide sequence from chromosome III of C. elegans. Nature *368*, 32–38.

Yau, K.-W. (1994). Cyclic nucleotide–gated channels: an expanding new family of ion channels. Proc. Natl. Acad. Sci. USA *91*, 3481–3483.

**GenBank Accession Number**

The accession number for the *tax-4* cDNA sequence reported in this paper is D86922.